Ionization of Ozone/Chlorofluorocarbon Mixtures in Atmospheric Gases: Formation and Remarkable Dissociation of $[CHXYO_3]^+$ Complexes (X = H, Cl, F; Y = Cl, F)

Fulvio Cacace,[a] Giulia de Petris,*[a] Federico Pepi,[a] Marzio Rosi,[b] and Anna Troiani[a]

Abstract: The reactions occurring upon ionization of mixtures containing ozone and CHX_2Y (X = H, Cl, F; Y = Cl, F) halocarbons diluted in atmospheric gases (O_2, N_2) have been investigated in detail by mass spectrometric and theoretical methods. In all systems investigated the reactivity pattern is characterized by the preliminary formation of $[CHXY \cdot O_3^+]$ adducts which undergo unimolecular dissociation into $HXYO_2^+$ and CO. This remarkable dissociation which requires extensive molecular reorganization is exceptional for hydrogenated halocarbons. The work represents the first systematic study of the ionic chemistry in systems containing both ozone and halocarbons diluted in atmospheric gases.

Keywords: atmospheric chemistry · gas-phase chemistry · ozone

Introduction

A vigorous research effort spanning more than four decades has brought into a sharp focus the key role played by ozone chemistry in the Earth's atmosphere. The discovery that the release of halocarbons to the troposphere seriously threatens the stratospheric ozone layer,[1] has heightened the awareness of the role played by minor atmospheric constituents in determining the natural ozone concentration. This has stimulated a thorough investigation of the detailed chemistry of halocarbons, demonstrating that hydrogenated molecules have a lower ozone depletion potential, traceable to their shorter lifetimes in the troposphere, where ozone remains of great interest, although a "minor" species in terms of abundance. The advances achieved in the understanding of the interactions between ozone and the halocarbons have chiefly concerned neutral species, although reactions involving ions have been shown to effectively produce or destroy neutral species, and ion chemistry is therefore important even in relation to neutral composition.[2] Recently, the ion chemistry of ozone[3, 4] as well as of ionized halocarbons in atmospheric gases[5, 6] have been studied separately. However, so far the nature and the effects of the *interactions* between ozone and the halocarbons in ionized mixtures have not been examined. Here we report a detailed study utilizing mass spectrometric and theoretical methods of the ionic reactions occurring in mixtures containing ozone and selected hydrogenated halocarbons diluted in atmospheric gases, such as O_2 or N_2. The results have disclosed the peculiar ionic reactivity of ozone towards this class of halocarbons, leading first to formation of charged ozone/halocarbenium ions complexes, followed by a remarkable reaction that eventually causes the extrusion of carbon monoxide. The results also point to the key role of the hydrogen atom in this class of processes.

[a] Prof. Dr. G. de Petris, Prof. Dr. F. Cacace, Dr. F. Pepi, Dr. A. Troiani
Dipartimento di Studi di Chimica e Tecnologia delle Sostanze Biologicamente Attive dell'Università "La Sapienza", P.le Aldo Moro 5, 00185 Roma (Italy)
Fax: (+39) 06 49913602
E-mail: depetris@axrma.uniroma1.it

[b] Prof. Dr. M. Rosi
Istituto per le Tecnologie Chimiche
Facoltà di Ingegneria, Università di Perugia
06100 Perugia (Italy)
Fax: (+39) 075 5855606

Supporting information for this contribution is available on the WWW under http://www.wiley-vch.de/home/chemistry/

Experimental Section

Mass spectrometric experiments: A ZABSpec oa-TOF with EBE TOF configuration, and a Fourier transform ion cyclotron resonance (FT-ICR) mass spectrometer were used to perform all reported experiments. The ions were generated in the high-pressure chemical ionization (CI) source of the ZABSpec mass spectrometer (Micromass Ltd.) under the following typical conditions: accelerating voltage 8 kV, emission current 0.5 mA, repeller voltage 0 V, and source temperature 150 °C. The mass-selected ions were structurally assayed by mass-analyzed ion kinetic energy (MIKE) and collisionally activated dissociation (CAD) mass spectrometry. In the latter case He was admitted into the collision cell at such a pressure as to reduce the intensity to 70 % of its original value. MS^3 experiments were performed by recording the CAD/TOF spectra of mass selected daughter ions from metastable decompositions, care being taken to avoid any contributions

  0947-6539/00/0614-2572 $ 17.50+.50/0 *Chem. Eur. J.* **2000**, *6*, No. 14

from collisionally induced dissociation. The FT-ICR experiments were performed with a Bruker Spectrospin Apex 47e instrument, equipped with an external CI source, a pulsed valve, a cylindrical "infinity" cell,[7] and a Bayard–Alpert ionization gauge, whose readings were corrected for its different sensitivity to the gases used.[8] The ions generated in the external ion source were transferred into the ICR cell and isolated by the standard procedure based on the "soft" ejection of all the unwanted ions. The ions were then allowed to react with the neutral reagent continuously admitted into the cell in order to reach stationary pressures ranging from 1×10^{-8} to 4×10^{-7} Torr. All the gases and the other chemicals utilized were research-grade products from commercial sources with a stated purity in excess of 99.99 mol% and were used without further purification. Ozone was synthesized by passing UHP grade oxygen (Matheson 99.95 mol%) through a commercial ozonizer, collected in a silica trap cooled to 77 K and released upon controlled warming of the trap.

Computational details: Density functional theory, based on the B3LYP functional,[9] was used to localize the stationary points of the investigated systems and to evaluate vibrational frequencies. Single point energy calculations at the optimized geometries were performed using the coupled-cluster single and double excitation method[10] with a perturbative estimate of the triple excitations according to the [CCSD(T)] approach.[11] Transition states were located using the synchronous transit-guided quasi Newton method from Schlegel and co-workers.[12] The 6-311G(d,p) basis set was used.[13]Zero-point energy (ZPE) corrections evaluated at B3LYP level were added to the CCSD(T) energies. The 0 K total energies of the species of interest were corrected to 298 K by adding translational, rotational, and vibrational contributions. The absolute entropies were calculated by using standard statistical-mechanistic procedures from scaled harmonic frequencies and moments of inertia relative to B3LYP/6-311G(d,p) optimized geometries. All calculations were carried out utilizing Gaussian 94.[14]

Results

Formation of the complexes: A number of $[CHXYO_3]^+$ (X = Cl, F, H; Y = Cl, F) adducts were generated in the source of the ZABSpec oa-TOF mass spectrometer from gaseous mixtures containing O_3, O_2 (or N_2), and CHX_2Y halocarbons. In particular, the following ions were obtained upon ionization of the following mixtures (in parentheses the species formed): $CHClF_2/O_3$ (**a**, **c**); $CHCl_2F/O_3$ (**a**, **b**); CHF_3/O_3 (**c**); CH_3F/O_3 (**d**). Ions **a** can be obtained from $CHClF_2/O_3$ and from $CHCl_2F/O_3$, whereas ion **c** can be obtained from $CHClF_2/O_3$ and CHF_3/O_3.

$CHClFO_3^+$ **a** $CHCl_2O_3^+$ **b** $CHF_2O_3^+$ **c** $CH_2FO_3^+$ **d**

Two major routes to ions **a**–**d** can be envisaged, namely the association of halocarbenium ions to ozone and ion-molecule reactions promoted by O_3^+.

Abstract in Italian: *Ioni [$CHXYO_3^+$] sono stati generati per ionizzazione di miscele contenenti ozono e alocarburi CHX_2Y (X = H, Cl, F; Y = Cl, F) diluite in gas atmosferici. Mediante tecniche spettrometriche di massa é stato dimostrato che la loro reattività é caratterizzata dalla dissociazione in $HXYO_2^+$ e CO. Questo processo richiede una estesa riorganizzazione molecolare ed é peculiare degli alocarburi idrogenati. Questo lavoro rappresenta il primo studio sistematico della chimica ionica di sistemi contenenti contemporaneamente ozono e alocarburi diluiti in gas atmosferici.*

As to the first route:

$$CHXY^+ + O_3 \longrightarrow \mathbf{a}, \mathbf{b}, \mathbf{c}, \mathbf{d} \quad (1)$$

the halocarbenium ions can be formed by direct fragmentation of halocarbons, or by ion-molecule reactions of the $CHXY^+$ ions, such as occurring in the halocarbons CI.[6]

$$CHClF_2 + CHF_2^+ \longrightarrow CHClF^+ + CHF_3 \quad (2)$$

$$CHCl_2F + CHClF^+ \longrightarrow CHCl_2^+ + CHClF_2 \quad (3)$$

As to the second general route, $CHXYO_3^+$ adducts can also be formed by O_3/CI of CHX_2Y accomplished at higher O_3/CHX_2Y ratios, where reactions (2) and (3) are completely suppressed. Under these conditions, ion **a** (from $CHCl_2F$), ion **c** (from $CHClF_2$), and ion **d** are the only $CHXYO_3^+$ adducts observed as the products from processes promoted by the O_3^+ ion:

$$O_3^+ + CHX_2Y \longrightarrow CHXY^+ + O_3 + X \longrightarrow CHXYO_3^+ + X \quad (4)$$

$$O_3^+ + CHX_2Y \longrightarrow CHX_2YO_3^+ + \longrightarrow CHXYO_3^+ + X \quad (5)$$

The occurrence of the dissociative charge transfer reaction (4) was demonstrated by FT-ICR experiments, where O_3^+ was produced in the external ion source and driven into the resonance cell in the presence of $CHClF_2$ and $CHCl_2F$ halocarbons. In the low pressure range (10^{-8} mbar) typical of the FT-ICR conditions one cannot detect the corresponding adducts. This is a result of their complete dissociation, whereas the more efficient collisional deactivation typical of a high pressure CI source allows survival of a fraction of $CHXYO_3^+$ adducts and hence occurrence of sequence (4).

Passing to process (5), detection of $CHX_2YO_3^+$ intermediates, such as **I** and **II**, in the O_3/CI of $CHClF_2$ and $CHCl_2F$ is mechanistically informative:

$$O_3^+ + CHClF_2 \longrightarrow \underset{\mathbf{I}}{CHClF_2O_3^+} \begin{cases} \not\rightarrow \mathbf{a} + F & (5a) \\ \rightarrow \mathbf{c} + Cl & (5c) \end{cases}$$

$$O_3^+ + CHCl_2F \longrightarrow \underset{\mathbf{II}}{CHCl_2FO_3^+} \begin{cases} \rightarrow \mathbf{a} + Cl & (5a') \\ \not\rightarrow \mathbf{b} + F & (5b) \end{cases}$$

The structural assay of **I** and **II** by MIKE spectrometry shows that **I** decomposes into ion **c** without formation of **a**, and **II** shows a major decomposition into ion **a**, without formation of **b**. Actually, when reactions (4) or (5) involve the breakage of the stronger C–F bond, they are expected to be overall endothermic, despite the exothermicity of their first step, the O_3^+/CHX_2Y charge transfer.[15] Likewise, these reactions are energetically unfavorable if CHX_2Y has a higher ionization potential than O_3, as in the case of CHF_3. Accordingly, only ions **a** from $CHCl_2F$, **c** from $CHClF_2$, and **d**

are formed by O_3/CI of CHX_2Y, due to the following reasons: i) at low partial pressures of CHX_2Y, the ion-molecule reactions (2) and (3) to **a** (from $CHClF_2$) and **b** are not significant, ii) the alternative reactions (4) and (5) to **a** (from $CHClF_2$) and **b**, as well as formation of **c** from CHF_3, are energetically unfavorable. Overall, the failure to detect **a** from $CHClF_2$, **c** from CHF_3 and **b** suggests that processes of type (4) and (5) prevail in the O_3/CI of CHX_2Y.

MIKE and CAD spectrometry: Ions **a–d** were structurally assayed by MIKE and CAD spectrometry, probing both the ^{35}Cl and ^{37}Cl isotopomers of ions, such as **a** and **b**, containing chlorine atoms. Table 1 reports the MIKE spectra, in which

Table 1. MIKE spectra of **a–d** ions from different reactions.

Ions	$CHClFO_3^+$ **a**		$CHCl_2O_3^+$ **b**	$CHF_2O_3^+$ **c**		$CH_2FO_3^+$ **d**
	$CHClF_2$	$CHCl_2F$		$CHClF_2$	CHF_3	
Fragment			Intensities (%)Σ			
$[M-O_3]^+$	5.8	9.4	93.2	13.1	11.2	
$[M-CO]^+$	89.6	86.1	6.8	45.6		33.4
$[M-HCl]^+$	4.6	4.4				
$[M-HF]^+$				4.6		41.7
$[HCO]^+$				36.7		24.9
$[FCO]^+$					66.4	
$[O_2H]^+$					22.3	

the fragments were assigned by combining the pieces of information derived from the spectra of the ^{37}Cl isotopomer and from the MS/MS experiments illustrated in the next paragraph. Representative spectra are illustrated in Figure 1.

The common feature of the MIKE spectra of these ions is a metastable decomposition, recently described in a preliminary report for ion **a**,[16] involving loss of CO.

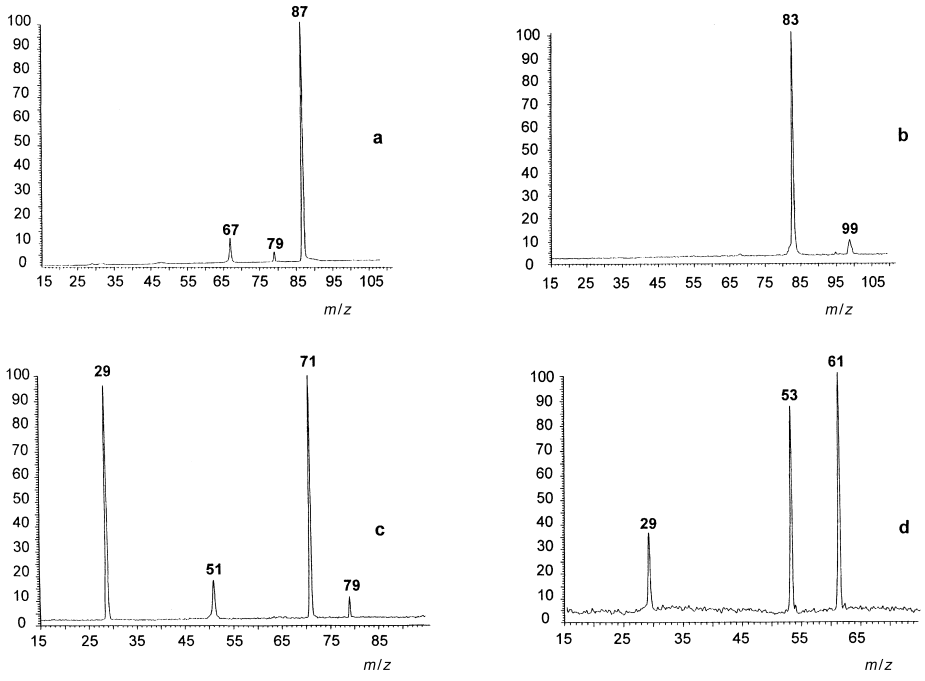

Figure 1. MIKE spectra of ions $CHClFO_3^+$ (a), $CHCl_2O_3^+$ (b), $CHF_2O_3^+$ from $CHClF_2$ (c), $CH_2FO_3^+$(d).

$$CHClFO_3^+ \ (\mathbf{a}) \rightarrow CHClF^+ + O_3 \quad (6a)$$
$$CHClFO_3^+ \ (\mathbf{a}) \rightarrow HClFO_2^+ + CO \quad (7a)$$
$$CHClFO_3^+ \ (\mathbf{a}) \rightarrow CFO_3^+ + HCl \quad (8a)$$

Irrespective of their source, ions **a** show closely similar MIKE spectra, characterized by the major transitions yielding the $[M-CO]^+$ ion, $HClFO_2^+$, as the most abundant fragment, the $[M-O_3]^+$ ion, $CHClF^+$, traceable to the back dissociation of the adduct, and a minor $[M-HCl]^+$ fragment, CFO_3^+.

$$CHCl_2O_3^+ \not\rightarrow CHCl_2^+ + O_3 \quad (6b)$$
$$CHCl_2O_3^+ \rightarrow HCl_2O_2^+ + CO \quad (7b)$$

The $CHCl_2O_3^+$ ions display a similar fragmentation pattern, although in this case reaction (6) predominates. The MIKE spectra of ions **c** are different, depending on the source of the population assayed. Thus, ions from $CHClF_2$ display the fragmentation pattern

$$CHF_2O_3^+ \ (\mathbf{c}, (CHClF_2)) \rightarrow CHF_2^+ + O_3 \quad (6c)$$
$$CHF_2O_3^+ \ (\mathbf{c}, (CHClF_2)) \rightarrow HF_2O_2^+ + CO \quad (7c)$$
$$CHF_2O_3^+ \ (\mathbf{c}, (CHClF_2)) \rightarrow CFO_3^+ + HF \quad (8c)$$
$$CHF_2O_3^+ \ (\mathbf{c}, (CHClF_2)) \rightarrow HCO^+ + [F_2, O_2] \quad (9c)$$

whereas those from CHF_3 undergo a different metastable decomposition:

$$CHF_2O_3^+ \ (\mathbf{c}, (CHF_2)) \rightarrow CHF_2^+ + O_3 \quad (6c)$$
$$CHF_2O_3^+ \ (\mathbf{c}, (CHF_2)) \rightarrow FCO^+ + [H, F, O_2] \quad (10c)$$
$$CHF_2O_3^+ \ (\mathbf{c}, (CHF_2)) \rightarrow O_2H^+ + [C, F_2, O] \quad (11c)$$

In the spectrum of **c** from $CHClF_2$ reactions (6) and (7) are the major processes, together with the minor fragmentation (8) and the formation of a fragment at $m/z = 29$. The spectrum of ions **c** from CHF_3 displays CHF_2^+ as the only common fragment, larger amounts of FCO^+ and O_2H^+ being detected. The latter two fragments are also present as small, but well detectable peaks, in the MIKE spectrum of $CHF_2O_3^+$ ions from $CHClF_2$, formed by mixtures containing a high $O_3/CHClF_2$ ratio.

Finally, the $CH_2FO_3^+$ ion **d** displays the fragmentation pattern:

$$CH_2FO_3^+ \ (\mathbf{d}) \rightarrow H_2FO_2^+ + CO \quad (7d)$$
$$CH_2FO_3^+ \ (\mathbf{d}) \rightarrow HCO_3^+ + HF \quad (8d)$$
$$CH_2FO_3^+ \ (\mathbf{d}) \rightarrow HCO^+ + [H, F, O_2] \quad (10d)$$

The CAD spectra are not particularly informative from the structural standpoint, in that the intensities of the few fragments not arising from metastable decompositions are relatively weak. Nevertheless, a significant piece

0947-6539/00/0614-2574 $ 17.50+.50/0 *Chem. Eur. J.* **2000**, *6*, No. 14

of information is that the CAD spectra of ions **a** are not affected by their source, whereas the spectra of ions **c** from $CHClF_2$ are markedly different from those of ions **c** from CHF_3. The latter ions show the weakest CAD spectrum, among those of the $CHXYO_3^+$ ions assayed, characterized by few and small CAD fragments (about 7% of the sum of the intensities) in addition to the metastable ones. Moreover, fragments typical of **c** from $CHClF_2$, such as $[M-CO]^+$, $[M-HF]^+$, etc., are absent in ions **c** from CHF_3, that displays a typical O_2H^+ CAD peak, absent in the CAD spectrum of ion **c** from $CHClF_2$.

MS³ experiments: In order to convalidate the assignment of the fragments observed in the MIKE spectra, confirmatory MS/MS experiments were performed where the daughter ions from the metastable decompositions were further probed by CAD, utilizing the TOF mass spectrometer, provided that their intensity is sufficiently high. When required the spectra of the ^{37}Cl isotopomers were also recorded. The obtained results are illustrated in Table 2.

Ions from dissociations (6a) and (6c) were identified as $CHClF^+$ and CHF_2^+, fully consistent with the suggested back dissociation of $CHXYO_3^+$ into $CHXY^+$ and O_3. Their spectra are similar to those of the model ions $CHFCl^+$ and CHF_2^+ obtained in the CI source from the ionization of neat $CHCl_2F$ and CHF_2Cl. No fragmentation is traceable to the presence of oxygen atoms in their structure, so that isobaric ions, for example ClO_2^+ and FO_2^+, can safely be ruled out.

Ions $HXYO_2^+$ from dissociation (7), assumed to involve CO loss, all decompose into YO_2^+ and HX, whereas ions CYO_3^+ from dissociation (8), assumed to involve HX loss, give YO_2^+ and CO, so that the following general pattern can be recognized, leading to YO_2^+ by two different routes:

$$CHXYO_3^+ \longrightarrow HXYO_2^+ + CO \rightarrow YO_2^+ + HX \quad (7)$$

$$CHXYO_3^+ \longrightarrow CYO_3^+ + HX \rightarrow YO_2^+ + CO \quad (8)$$

Computational results: Tables 3–6 report the total energies of the investigated systems for the study of the potential energy surface (PES) of ions **a**, **b**, **c**, and **d** computed at B3LYP and CCSD(T) level. Table 7 illustrates the energetics of related processes, computed at the CCSD(T) level, whereas the zero point energies and the thermal corrections were evaluated at B3LYP/6-311G(d,p) level.

Table 2. MS/MS spectra of ions from decompositions of $CHXYO_3^+$.

Parent ion	Reaction	Daughter ion (m/z)	Fragment m/z (intensity %)	Assignment
$CHClFO_3^+$ (**a**)	6a	67	48 (12.8), 47 (10.7) 32 (31.0), 31 (45.5)	**a** → $CHClF^+$ → CCl^+, $CHCl^+$, CF^+, CHF^+
m/z 115	7a	87, 89	67, 69 (59), 51 (41)	**a** → $HFClO_2^+$ → ClO_2^+, FO_2^+
m/z 117	8a	79	51 (100)	**a** → CFO_3^+ → FO_2^+
$CHF_2O_3^+$ (**c**)	6c	51	32 (30.6), 31 (69.4)	**c** → CHF_2^+ → CF^+, CHF^+
	7c	71	51 (100)	**c** → $HF_2O_2^+$ → FO_2^+
m/z 99	8c	79	51 (100)	**c** → CFO_3^+ → FO_2^+
$CH_2FO_3^+$ (**d**) m/z 81	7d	53	33 (100)	**d** → $H_2FO_2^+$ → O_2H^+
	8d	61	33 (100)	**d** → HCO_3^+ → O_2H^+

Table 3. Total energies (hartree) of the investigated systems for the study of the PES of ion **a**.

	E_{B3lyp}	ZPE	$E_{CCSD(T)}$
1a	−823.917763	0.029378	−822.569778
2a	−823.980143	0.028924	−822.619820
3a	−823.962498	0.024747	−822.619252
4a	−823.964566	0.024340	−822.618447
2a′	−823.920165	0.028127	−822.563500
3a′	−823.918798	0.021910	−822.567717
4a′	−823.909874	0.022078	−822.561612
TS(**1a** → **2a**)	−823.905540	0.027114	−822.558591
TS(**2a** → **3a**)	−823.931662	0.024029	−822.574928
TS(**3a** → **4a**)	−823.955113	0.023659	−822.614810
TS(**1a** → **2a′**)	−823.867900	0.026799	−822.527415
TS(**2a′** → **3a′**)	−823.913065	0.026113	−822.553808
TS(**3a′** → **4a′**)	−823.893246	0.021191	−822.543995
$CHClF^+$	−598.425982	0.019134	−597.570068
$HFOOCl^+$	−710.596429	0.017636	−709.515328
$HFClOO^+$	−710.597769	0.017354	−709.516639
$HClOOF^+$	−710.551359	0.015941	−709.459703
$HClFOO^+$	−710.547346	0.015101	−709.462470
ClO_2^+	−610.099725	0.005931	−609.225177
FO_2^+	−249.663319	0.007133	−249.16457
HFCO	−213.831232	0.020809	−213.364169
HClCO	−574.180041	0.019024	−573.342396
O_3	−225.470793	0.007267	−224.987776
HF	−100.469728	0.009383	−100.273729
HCl	−460.833471	0.006695	−460.263272
CO	−113.346236	0.005059	−113.092795

Table 4. Total energies (hartree) of the investigated systems for the study of the PES of ion **b**.

	E_{B3lyp}	ZPE	$E_{CCSD(T)}$
1b	−1184.275074	0.027690	−1182.561624
2b	−1184.333513	0.026943	−1182.604640
3b	−1184.331349	0.021038	−1182.610326
4b	−1184.328361	0.021091	−1182.605008
TS(**1b** → **2b**)	−1184.270540	0.026794	−1182.555605
TS(**2b** → **3b**)	−1184.316667	0.022775	−1182.591837
TS(**3b** → **4b**)	−1184.321894	0.020495	−1182.603872
$CHCl_2^+$	−958.792814	0.017508	−957.570103
$HClOOCl^+$	−1070.968853	0.014646	−1069.505158
$HClClOO^+$	−1070.967432	0.014374	−1069.506272
ClO_2^+	−610.099725	0.005931	−609.225177
HClCO	−574.180041	0.019024	−573.342396
O_3	−225.470793	0.007267	−224.987776
HCl	−460.833471	0.006695	−460.263272
CO	−113.346236	0.005059	−113.092795

Figure 2 shows the optimized geometries of the minima localized on the PES of the $CHClFO_3^+$ ion **a**. Structure **1a** can be described as a tetrahedral C atom bonded to Cl, F, and H atoms and to a slightly distorted ozone molecule. It lies below the energy of $CHClF^+ + O_3$ by 6.1 kcal mol^{-1} that corresponds to the association energy. Ion **2a**, more stable than **1a** by 31.8 kcal mol^{-1}, is viewed as a formyl fluoride molecule which interacts electrostatically with a ClO_2^+ fragment. Ions **3a** and **4a** represent the products of two different geometrical rearrangements of **2a**:**3a** is an almost linear OCHF species

Table 5. Total energies (hartree) of the investigated systems for the study of the PES of ion **c**.

	E_{B3lyp}	ZPE	$E_{CCSD(T)}$
1c	−463.565049	0.031154	−462.590763
2c	−463.564561	0.030157	−462.575373
3c	−463.543260	0.025538	−462.571789
4c	−463.534244	0.025149	−462.561446
5c	−463.673851	0.031602	−462.702805
6c	−463.642463	0.028559	−462.668564
7c	−463.641293	0.029960	−462.658730
TS(**1c**→**2c**)	−463.514154	0.029637	−462.537021
TS(**2c**→**3c**)	−463.522470	0.025482	−462.539328
TS(**3c**→**4c**)	−463.526818	0.024809	−462.559563
TS(**1c**→**5c**)	−463.547624	0.026739	−462.568795
TS(**5c**→**6c**)	−463.631514	0.027751	−462.658439
TS(**6c**→**7c**)	−463.630790	0.026815	−462.638439
CHF_2^+	−238.063157	0.021022	−237.575775
$HFOOF^+$	−350.171524	0.018898	−349.460395
$HFFOO^+$	−350.156147	0.018263	−349.450427
FO_2^+	−249.663319	0.007133	−249.164574
O_2H^+	−150.510161	0.013955	−150.203444
HFCO	−213.831232	0.020809	−213.364169
F_2CO	−313.106496	0.014021	−312.450167
O_3	−225.470793	0.007267	−224.987776
HF	−100.469728	0.009383	−100.273729
CO	−113.346236	0.005059	−113.092795

Table 6. Total energies (hartree) of the investigated systems for the study of the PES of ion **d**.

	E_{B3lyp}	ZPE	$E_{CCSD(T)}$
1d	−364.306632	0.039096	−363.522230
2d	−364.409703	0.039548	−363.612050
3d	−364.390620	0.034558	−363.604807
4d	−364.397197	0.031798	−363.624947
5d	−364.412636	0.039307	−363.629440
6d	−364.395880	0.033923	−363.617464
TS(**1d**→**2d**)	−364.296105	0.034400	−363.506426
TS(**2d**→**3d**)	−364.377996	0.031316	−363.596589
TS(**1d**→**5d**)	−364.282221	0.032195	−363.492238
TS(**5d**→**6d**)	−364.325849	0.032531	−363.542019
TS(**5d**→**4d**)	−364.393801	0.031456	−363.626919
CH_2F^+	−138.780095	0.026880	−138.481828
$HFOOH^+$	−251.019297	0.027637	−250.495894
O_2H^+	−150.510161	0.013955	−150.203444
HFCO	−213.831232	0.020809	−213.364169
O_3	−225.470793	0.007267	−224.987776
HF	−100.469728	0.009383	−100.273729
CO	−113.346236	0.005059	−113.092795

interacting with a ClO_2^+ fragment, whereas **4a** shows the ClO_2 unit centrally bound to the HF and CO moieties. Ions **3a** and **4a** are more stable than **1a** by 32.6 and 31.8 kcal mol^{-1}, respectively. Figure 2 also reports the optimized geometries of the less stable ions **2a′**, **3a′**,and **4a′**. Ion **2a′** is formed by a formyl chloride interacting with a FO_2^+ fragment, **3a′** is a linear OCHCl unit interacting with a FO_2^+ fragment and **4a′** displays the HCl–FO_2–CO connectivity.

Figure 3 shows the optimized geometries of the minima localized on the PES of the $CHCl_2O_3^+$ ion **b**. Structure **1b** can be described as a tetrahedral carbon bonded to two chlorine atoms, a hydrogen atom and an ozone molecule, whose geometry is only slightly distorted and bent toward the carbon. It lies only 1 kcal mol^{-1} below the energy of $CHCl_2^+$+O_3. Ion **2b**, formed by a formyl chloride molecule

Table 7. Thermochemical data (kcal mol^{-1}, 298 K) relevant to the PES of ions **a**, **b**, **c**, and **d** computed at the CCSD(T) level of theory.

Process	ΔH^0_{298}	Barrier height
$CHClF^+$+O_3→**1a**	−6.1	
1a→**2a**	−31.8	5.5
2a→**3a**	−0.8	26.1
3a→**4a**	0.8	2.4
1a→**2a′**	3.6	24.8
2a′→**3a′**	−5.8	5.0
3a′→**4a′**	4.7	15.1
$CHCl_2^+$+O_3→**1b**	−1.0	
1b→**2b**	−27.0	2.8
2b→**3b**	−6.4	6.0
3b→**4b**	4.0	4.0
CHF_2^++O_3→**1c**	−17.3	
1c→**2c**	10.9	33.7
2c→**3c**	0.0	20.0
3c→**4c**	7.1	7.6
1c→**5c**	−68.2	12.5
5c→**6c**	20.2	25.8
6c→**7c**	6.7	17.0
CH_2F^++O_3→**1d**	−30.9	
1d→**2d**	−55.7	6.9
2d→**3d**	2.2	4.7
1d→**5d**	−68.1	14.6
5d→**4d**	−1.0	0.4
5d→**6d**	6.7	50.6

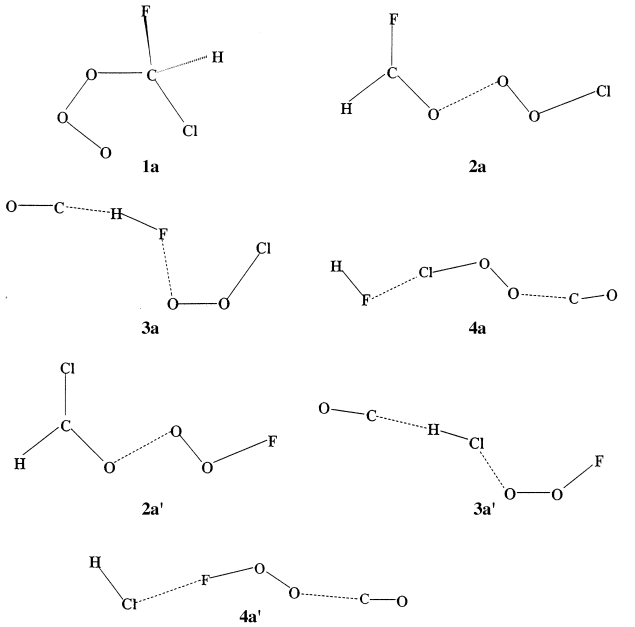

Figure 2. Structure of relevant minima in the $CHClFO_3^+$ system. The detailed geometrical parameters in this and the following figures are available as Supporting Information.

interacting electrostatically with a ClO_2^+ fragment, is more stable than **1b** by 27.0 kcal mol^{-1}, whereas ions **3b** and **4b** are more stable than **1b** by 33.4 and 29.4 kcal mol^{-1}, respectively. Ion **3b** is formed by an almost linear OCHCl system interacting with a ClO_2^+ fragment, and **4b** shows a central ClO_2 unit bound to the HCl and CO moieties.

Figure 4 shows the optimized geometries of the minima localized on the PES of the $CHF_2O_3^+$ ion **c**. Structure **1c** can be described as containing a tetrahedral carbon bonded to two

0947-6539/00/0614-2576 $ 17.50+.50/0 *Chem. Eur. J.* **2000**, *6*, No. 14

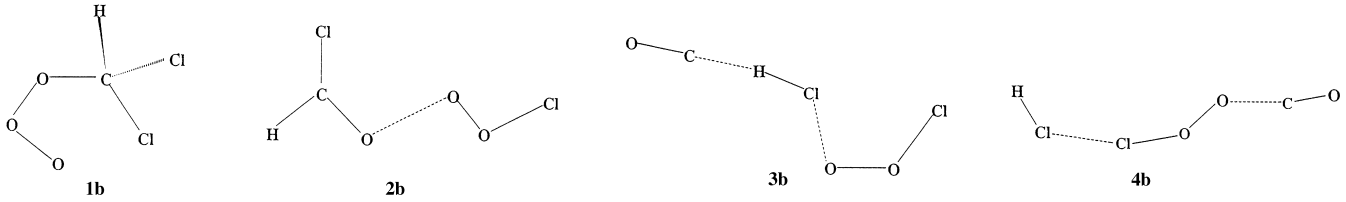

Figure 3. Structure of relevant minima in the $CHCl_2O_3^+$ system.

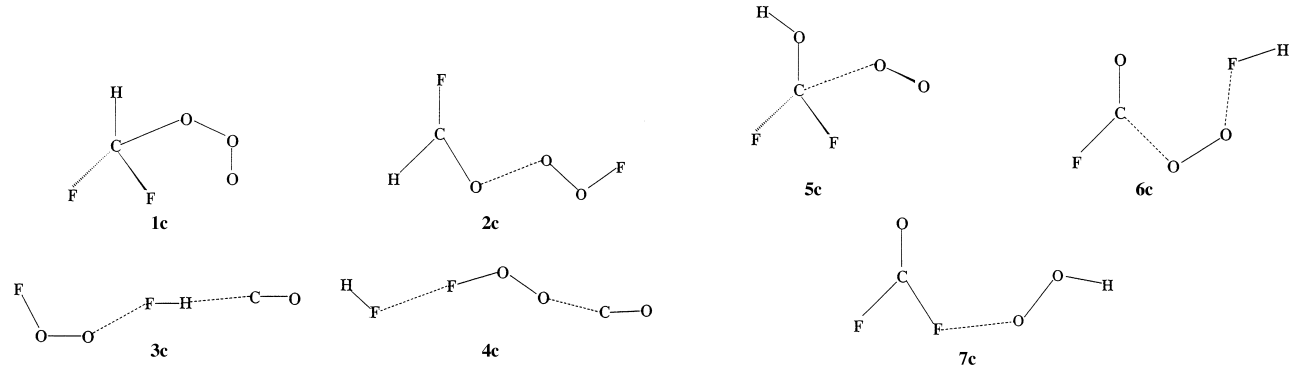

Figure 4. Structure of relevant minima in the $CHF_2O_3^+$ system.

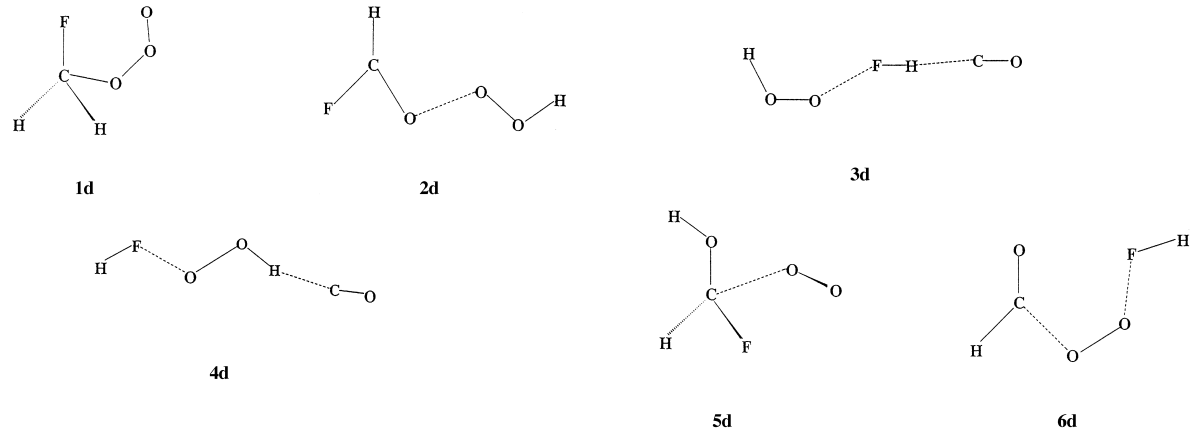

Figure 5. Structure of relevant minima in the $CH_2FO_3^+$ system.

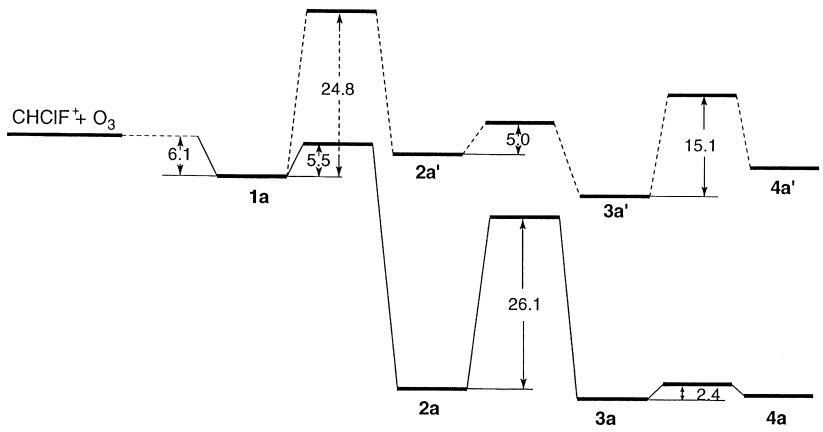

Figure 6. Energy profile for the $CHClF^+ + O_3$ system. Complete energetic details for this and the other systems are given in Table 7.

fluorine atoms, an hydrogen and a slightly distorted ozone molecule. It lies 17.3 kcal mol^{-1} below the energy of $CHF_2^+ + O_3$. Ion **2c**, the structure containing a formyl fluoride interacting with a FO_2^+ fragment, is less stable than **1c** by 10.9 kcal mol^{-1}. Ions **3c** and **4c** are less stable than **1c** by 10.9 and 18.0 kcal mol^{-1}, respectively, and are structurally similar to the **3** and **4** ions examined so far. Much more stable ions are **5c**, **6c**, and **7c**, lower in energy than **1c** by 68.2, 48.0, and 41.3 kcal mol^{-1}, respectively.

Figure 5 shows the optimized geometries of the minima localized on the PES of the $CH_2FO_3^+$ ion **d**. Structure **1d** can be described as containing a tetrahedral carbon bonded to

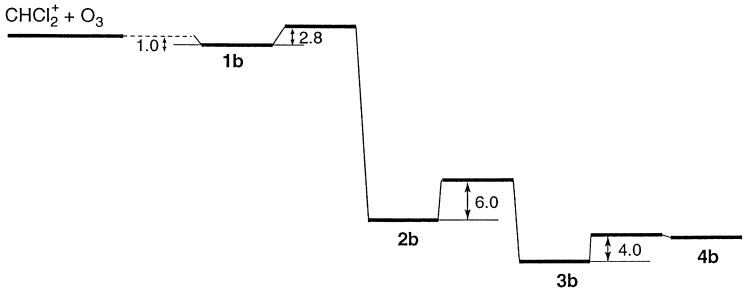

Figure 7. Energy profile for the $CHCl_2^+ + O_3$ system.

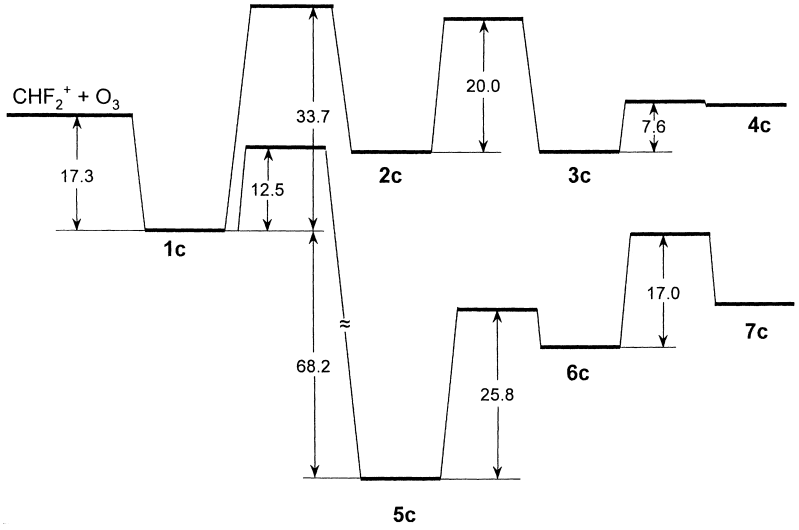

Figure 8. Energy profile for the $CHF_2^+ + O_3$ system.

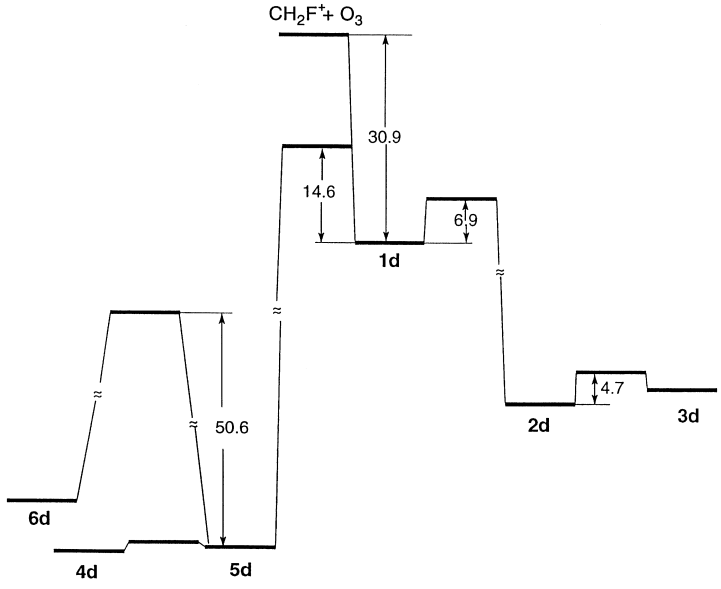

Figure 9. Energy profile for the $CH_2F^+ + O_3$ system.

two hydrogen and one fluorine atoms, and a slightly distorted ozone molecule. It lies 30.9 kcal mol^{-1} below the energy level of $CH_2F^+ + O_3$. Ion **2d**, whose structure contains a formyl fluoride interacting with the O_2H^+ fragment, and **3d**, the linear OCHF species interacting with O_2H^+, are more stable than **1d** by 55.7 and 53.5 kcal mol^{-1}, respectively. Other minima are ions **5d** and **6d**, more stable than **1d** by 68.1 and 61.4 kcal mol^{-1}, respectively, and structurally similar to **5c** and **6c**. At variance with the systems so far investigated, ion **4d** is more stable than **3d** by 15.6 kcal mol^{-1}, and derives from a rearrangement of **5d** rather than from the **1** → **2** → **3** pathway. Moreover, the orientation of the O_2H^+ ion within the complex slightly differs from that of the ClO_2^+ and FO_2^+ ions within the **4a–4c** complexes, in that it binds the carbon atom of CO by the hydrogen atom rather than by the oxygen atom. The energy profiles of the systems investigated are reported in Figures 6–9.

Discussion

The extrusion of carbon monoxide: All the $CHXYO_3^+$ ions investigated display a truly remarkable process, the metastable decomposition (7) into $HXYO_2^+$ and CO, that requires fission of all the C–H, C–F, and C–Cl bonds initially present in the CHXY moiety. Such a profound molecular reorganization makes this unimolecular fragmentation exceptional in the general reactivity pattern shown by O_3 in the gas-phase. The O-donor character of O_3 toward neutral and ionic species is well documented,[17, 4] and recently fragmentation processes have been found to occur in charged complexes of ozone with biatomic AB^+ ions:[18]

$$O_3 + {}^{18}O_2^+ \longrightarrow O_3{}^{18}O_2^+ \longrightarrow O^{18}O^+ \quad (12)$$

$$O_3 + NF^+ \longrightarrow O_3NF^+ \longrightarrow NO^+ \quad (13)$$

$$O_3 + Cl_2^+ \longrightarrow O_3Cl_2^+ \longrightarrow ClO^+ \quad (14)$$

where the O_3 moiety undergoes O_2 and O transfer to the A or B atom of AB^+.

$$O_3 + AB^+ \longrightarrow O_3A\text{----}B^+ \longrightarrow AO(AO^+) + BO_2^+(BO_2) \quad (15)$$

As a consequence, the A–B bond is broken, and A and B are separated and incorporated into two species, the one characterized by the lower ionization potential carrying the positive charge. In a quite similar way, one can regard $CHXY^+$ as an AB^+ ion, where A is the carbon atom, and all other atoms are the B moiety. According to the general scheme depicted in Equation (15), all the AH, AX and AY bonds are broken and the subsequent reorganization has the effect to bind together the H, X, and Y atoms into a single BO_2^+ ion.

$$O_3 + CHXY^+ \longrightarrow O_3CHXY^+ \longrightarrow CO + HXYO_2^+ \quad (16)$$

Support to such an intriguing generalization is lended by the MS^3 experiments illustrated in Table 2. Their results show

0947-6539/00/0614-2578 $ 17.50+.50/0 *Chem. Eur. J.* **2000**, *6*, No. 14

that decompositions (7) and (8) lead to the common final product, YO_2^+.

$$CHXYO_3^+ \longrightarrow CO + HXYO_2^+ \longrightarrow YO_2^+ + HX \quad (7)$$

$$CHXYO_3^+ \longrightarrow HX + COYO_2^+ \longrightarrow YO_2^+ + HX \quad (8)$$

As a matter of fact, most of the $CHXYO_3^+$ adducts either first loose CO, then HX, or first HX, then CO. This would suggest that a complex does exist that contains the YO_2, CO, and HX moieties

$$[YO_2, CO, HX]^+$$

and that it evolves into a YO_2^+ ion associated either to HX or to CO.

Moreover, experiments performed by assaying the $CX_2YO_3^+$ adducts by MIKE-CAD spectrometry show that they never decompose into $X_2YO_2^+$ and CO. This underlines the key role played by the hydrogen atom, capable of forming the polar HX molecule, that is essential to stabilize the complex. Formation of HX also provides the driving force for

$$O_3{+}CHXY{+} \longrightarrow [O_3{-}C(HX)Y]^+ \longrightarrow [YO_2, CO, HX]^+ \quad (17)$$

the process reminescent of reaction (15). In this reaction O_3 gives its O and O_2 units to the C and the Y atoms, causing the fission of the C–Y bond, and formation of the CO and YO_2 moieties.

The theoretical investigation of the potential energy surfaces of ions **a–d** suggests a reaction pathway quite consistent with the above picture. As shown in the energy profiles of Figures 6–9, in order to undergo CO loss ions **1a–1d** must isomerize to species of suitable configuration, such as ions **3** and/or **4** (Figures 2–5). In ion **3**, of OC-HX-OOY connectivity, the polar HX moiety holds together CO and YO_2, whereas ion **4** displays the alternative HX-YOO-CO connectivity. Based on their geometrical features, ions **3** and **4** can reasonably be regarded as electrostatic complexes, containing different arrangements of the HX, CO, and YO_2 moieties, all liable to the CO loss (7); the computed endothermicities are reported in Table 8. Isomerization to ions **3** and **4** occurs through the $YOOOCHX^+$ ions **2** (Figures 2–5), the preliminary breaking of the C–Y bond thus representing the first step of the **1** → **2** → **3(4)** → $HXYO_2^+$+CO sequence.

Table 8. Enthalpy changes of the processes leading to CO loss (kcal mol^{-1}, 298 K), computed at the CCSD(T) level of theory.

Process	ΔH^0 change
3a → $HFOOCl^+$+CO	6.2
4a → $HFClOO^+$+CO	4.0
3a′ → $HClOOF^+$+CO	9.5
4a′ → $HClFOO^+$+CO	2.9
3b → $HClOOCl^+$+CO	7.3
4b → $HClClOO^+$+CO	2.7
3c → $HFOOF^+$+CO	11.3
4c → $HFFOO^+$+CO	10.4
3d → $HOOFH^+$+CO	9.5
4d → $HOOFH^+$+CO	23.5

Table 9. Comparison of the barrier heights of selected processes (kcal mol^{-1}, 298 K) computed at the CCSD(T) level of theory.

Process	Barrier height
1 → **2**	
1a → **2a**	5.5
1b → **2b**	2.8
1d → **2d**	6.9
1c → **2c**	33.7
1a → **2a′**	24.8
2 → **3**	
HFCO → CO+HF	51.9
2a → **3a**	26.1
2c → **3c**	20.0
HClCO → CO+HCl	38.1
2b → **3b**	6.0
2a′ → **3a′**	5.0

For comparative purposes, the barriers for the **1** → **2** and **2** → **3** isomerizations are summarized in Table 9. The **1** → **2** isomerization of ions **a**, **b**, and **d** is characterized by much lower barriers than that of ion **c**, as expected if comparing the relative strenght of the C–Cl and C–H bonds to that of a C–F bond. Note that formation of **2a′** ($FOOOCHCl^+$), that differs from **2a** ($ClOOOCHF^+$) as to the location of the halogen atoms, again involves migration of a fluorine atom, and accordingly the barrier rises from 5.5 to 24.8 kcal mol^{-1}. It follows that the preliminary **1** → **2** isomerization becomes the step critical in determining the efficiency of the whole sequence.

As to the **2** → **3** isomerizations, they correspond to the decomposition of a formyl halide molecule in the presence of a ClO_2^+, or a FO_2^+ ion. In Table 9 the barriers for these isomerizations are compared with those computed for the decompositions of isolated HFCO and HClCO, and result considerably lower, due to the solvating effect of YO_2^+.

$CHFClO_3^+$: The energy profile reported in Figure 6, relevant to the PES of $CHClFO_3^+$, shows a branching of the reaction pathway to ions **2**, **3**, and **4**. The presence of two different halogen atoms in $CHClFO_3^+$ originates mirror ion pairs **2a–2a′**, **3a–3a′**, and **4a–4a′**, whose partners differ as to the respective location of the halogen atoms (Figure 2). Ions **a** are much more stable than ions **a′** (Table 7), since they contain the more polar HF moiety rather than HCl, and the whole **2a′** → **4a′** path lies higher in energy with respect to the **2a** → **4a** path. To estimate the energy excess imparted to the $CHXYO_3^+$ ions by the formation processes, the exothermicity of reactions (1)–(5) can be evaluted for all the **a–d** ions, combining available thermochemical data[15] with the computed association energies of $CHXY^+$ and O_3. Reaction (1) is calculated to be exothermic by 6.1 kcal mol^{-1} for ions **a**; reaction (2), the first step to **a** from $CHClF_2$, is evaluated to be exothermic by 18.4 kcal mol^{-1}, and reactions (4) or (5), the additional routes from $CHCl_2F$ to **a**, are exothermic by 19.1 kcal mol^{-1}. Therefore **1a** can isomerize to the more stable **2a** or back dissociate to the reactants by energetically comparable processes (Figure 6), and the **1a** → **4a** pathway, whose barrier is located below the internal energy excess imparted by the formation

reactions, makes the loss of carbon monoxide a possible decomposition channel from low energy ions as well. The formation reactions employed allow both pathways from **2** to **4**, generating ions that have a sufficient energy content to overcome the **1a** → **2a′** barrier. The experimental evidence, in particular the evidence from fragmentation processes (7) and (8), suggests the existence of ions of both connectivities **a** and **a′** within the metastable ionic population. Indeed, the MS^3 spectrum of ions from (7a) shows both the FO_2^+ and ClO_2^+ fragments (Table 2), pointing to the presence of two different ions, that is $HClFO_2^+$ and $HFClO_2^+$, in the populations probed. Yet, the metastable decomposition (8a), admittingly a minor process (Table 1), can only be traced to a structure, as for example **3a′** or **4a′**, containing a distinct HCl moiety.

$CHCl_2O_3^+$: Reaction (3), the first step to formation of **b**, is exothermic by 14.6 kcal mol^{-1}, and the association energy computed for $CHCl_2O_3^+$ is just 1 kcal mol^{-1}. As ion **a**, $CHCl_2O_3^+$ also decomposes through **2b**. The shallower energy well of **1b** than of **1a** (Figures 6, 7) accounts for the higher efficiency of the back dissociation reaction (6b) and for the lower intensity of the $[M-CO]^+$ fragment (7b) observed in the MIKE spectrum of **b**.

$CHF_2O_3^+$: The evidence from MIKE and CAD spectrometry indicates different ionic populations of ions **c**, depending on their source and hence on the different exothermicity of their formation reactions. Actually, whereas reaction (1) is computed to be exothermic by 17.3 kcal mol^{-1} for ion **c** (Table 7), the internal energy excess of the CHF_2^+ reactant ions can be different, when $CHClF_2$ or CHF_3 are utilized as the precursor. Indeed, CHF_2^+ ions from $CHClF_2$ can undergo reaction (2) with $CHClF_2$ yielding the $CHClF^+$ ion, and the CHF_2^+ ions that escape this efficient process can have a large excess of internal energy. CHF_2^+ ions from CHF_3 are instead thermalized by multiple collisions with the bath gas, since the thermoneutral reaction has the only effect to stabilize CHF_2^+, and ions **c** formed in this way can be identified as the $CHF_2O_3^+$ population of lowest energy content.

$$CHF_2^+ + CHF_3 \longrightarrow CHF_3 + CHF_2^+ \qquad (18)$$

As previously illustrated, the **1** → **2** isomerization is the crucial step for the formation of ions **3** and **4**, and hence the loss of CO can strongly be affected by the energetics of the formation process of **1**, if prior isomerization to **2** is particularly slow. In this case, the **1c** → **2c** barrier is higher than in the case of ions **a**, **b**, and **d** (Figure 8), and formation reactions of different exothermicity are available. Accordingly, ions **c** from $CHClF_2$ undergo dissociation to $HF_2O_2^+$ and CO, whereas the colder ions **c** from CHF_3 cannot overcome the **1c** → **2c** barrier and display no such decomposition. The difference is particularly relevant owing to the existence of an energetically less demanding reaction pathway. As shown in Figure 8, a low barrier, quite below the dissociation threshold, separates **1c** from the minimum **5c**, the most stable ion on the PES of **c**. The facile isomerization to **6c** and **7c** accounts for the FCO^+ [reaction (10c)] and O_2H^+ [reaction (11c)] fragments observed in the MIKE spectrum of **c** from CHF_3. These fragments, absent in the MIKE spectrum of ions **c** from $CHClF_2$, appear in the population obtained from the O_3/CI of $CHClF_2$, suggesting that under these conditions a milder process contributes to the formation of **c**. Indeed, reactions (4) or (5) estimated to be exothermic by about 13 kcal mol^{-1}, provide in these experiments a different route to ions **c.** Reaction (1) from excited CHF_2^+ ions not stabilized by collisions with the bath gas molecules (O_3/O_2), can still be efficient, thus explaining the observation of the fragmentation pattern typical of **c** from $CHClF_2$. Finally, the CAD spectra, showing well distinguishable populations of stable ions, reinforce the evidence for two different reaction pathways.

$CH_2FO_3^+$: Among the investigated $CHXYO_3^+$ ions, $CH_2FO_3^+$ is characterized by the deepest energy well. The computed value of 30.9 kcal mol^{-1} reasonably accounts for the absence of the decomposition reaction (6) from ions **d** (Table 1). The energy profile, lying much below the energy level of the reactants (Figure 9), and the presence of two hydrogen atoms cause the ion **d** to combine the different features noted for ions **a**–**c**. Two different paths can be recognized, the **1** → **3** path, common to ions **a**–**c**, that leads to CO loss (7–8d), and the **1** → **6** path leading to HCO^+ (10d), also observed from ion **c**. In this connection, as shown in Figures 4 and 5, the similarity of ions **5**–**6d** and **5**–**6c**, where a fluorine atom bound to the carbon is replaced by an hydrogen atom, accounts for the occurrence of the **1** → **6** path to yield the FCO^+ fragment from ion **c** [reaction (10c)], and the HCO^+ fragment from ion **d** [reaction (10d)]. However, at variance with the case of ion **c**, the two paths available to ion **d** are characterized by comparable barriers, both located below the association energy value of **1d**, and thus accessible to ions of widely different energy content. Even the barrier for the **5** → **6** isomerization, involving fission of the C–F bond, and therefore as high as 50.6 kcal mol^{-1}, is located about 48 kcal mol^{-1} below the dissociation threshold, due to the deep wells of ions **1d** and **5d**. Yet, the **1** → **2** → **3** path of ion **d** does not generate ions of type **4**, conversely the **1** → **5** path, leading to structures containing O_2 moieties, proves a convenient route to ions **4** and therefore an alternative path to CO loss. This can be rationalized considering that, owing to the presence of two hydrogen atoms in $CH_2FO_3^+$, formation of HF, that represents the driving force of the process, results in the formation of the O_2H^+ ion, that happens to be generated in the **1** → **5** path as well.

Noteworthy is also the peculiarity of the $CHF_2O_3^+$ and $CH_2FO_3^+$ systems, displaying two reaction paths, the one to the $[HX, YO_2, CO]^+$ complexes, and the other to the **5**–**7** structures containing a distinct O_2 moiety. Actually, the theoretical investigation of the PES of $CHClFO_3^+$ and $CHCl_2O_3^+$ has identified stable minima whose structures contain a distinct O_2 moiety (see Figure 10).

Whereas these are much more stable than ions **2**–**4**, as in the case of ions **c** and **d**, the barriers for the isomerization of **1a** and **1b** into these minima are as high as

0947-6539/00/0614-2580 $ 17.50+.50/0 *Chem. Eur. J.* **2000**, *6*, No. 14

60 kcal mol^{-1}, which makes them undetectable in our experimental conditions; this is a result of the insufficient exothermicity of the formation processes employed. Such a difference can be traced to the different nature and number of bonds broken in the isomerization process, severely affected by the presence of strong C–F bonds. Indeed, the **1** → **5** process that generates the O_2 unit is followed by the **5** → **6** isomerization that breaks the C–F bond, whereas the **a** and **b** structures of Figure 10 are formed by processes that require the simultaneous rupture of a C–Cl bond and an O–O bond of ozone, and therefore are characterized by much higher barriers.

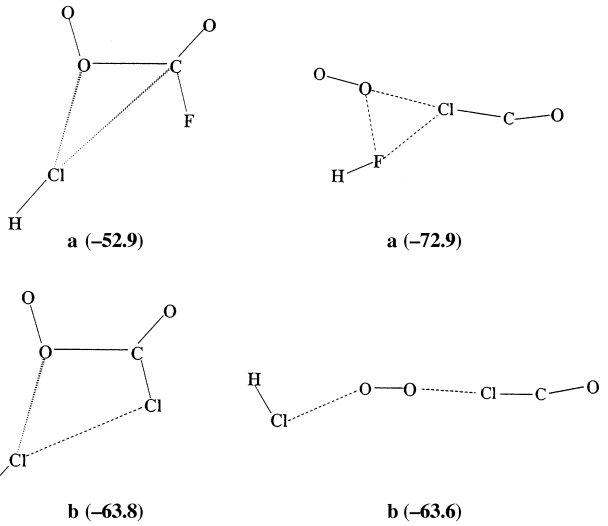

Figure 10. Structures of ions **a** and **b**, and relative energies with respect to **1a** and **1b** (see text).

Conclusion

The $CHXYO_3^+$ adducts, generated in ionized mixtures of ozone and hydrogenated halocarbons, CHX_2Y, show a common metastable decomposition into $HXYO_2^+$ and CO, that requires profound molecular reorganization and isomerization (**1** → **4**) into [HX, YO_2, CO]$^+$ complexes. Such a behavior is peculiar of hydrogenated halocarbons, since the presence of at least one hydrogen atom plays a key role in the process. $CHF_2O_3^+$ and $CH_2FO_3^+$ ions show an additional decomposition pattern, traceable to the **1** → **6** isomerization process to species containing a distinct O_2 unit. Based on the energetics of the formation process one can discriminate between the two fragmentation routes of the $CHF_2O_3^+$ ion, the **1** → **4** and **1** → **6** paths being characterized by barriers of different height. Conversely, in the case of $CH_2FO_3^+$ ions, the barriers of the two paths are located well below the energy level of the $CH_2F^+ + O_3$ system, and hence both the isomerization processes are accessible to ions **d** irrespective of their internal energy excess.

Acknowledgement

The financial support of the University of Rome "La Sapienza", the University of Perugia, Consiglio Nazionale delle Ricerche (CNR), Ministero dell'Università e della Ricerca Scientifica e Tecnologica (MURST) is gratefully acknowledged. The authors express their gratitude to R. Cipollini and A. Sgamellotti for their active interest in this work, and to E. Floridi and M. Di Stefano for their assistance in some of the computations.

[1] M. J. Molina, F. S. Rowland, *Nature* **1974**, *249*, 810.
[2] D. Smith, P. Spanel, *Mass Spectrom. Rev.* **1995**, *14*, 255, and references therein.
[3] F. Cacace, M. Speranza, *Science* **1994**, *265*, 208.
[4] M. A. Mendes, L. A. B. Moraes, R. Sparrapan, M. N. Eberlin, R. Kostiainen, T. Kotiaho, *J. Am. Chem. Soc.* **1998**, *120*, 7869.
[5] R. A. Morris, A. A. Viggiano, S. T. Arnold, J. F. Paulson, J. F. Liebman, *J. Phys. Chem.* **1995**, *99*, 5992.
[6] A. B. Raksit, *Int. J. Mass Spectrom. Ion Processes* **1986**, *69*, 45.
[7] P. Caravatti, M. Allemann, *Org. Mass Spectrom.* **1991**, *26*, 514.
[8] J. E. Bartmess, R. M. Georgiadis, *Vacuum* **1983**, *33*, 149.
[9] a) P. J. Stevens, F. J. Devlin, C. F. Chabalowski, M. J. Frisch, *J. Phys. Chem.* **1994**, *98*, 11623; b) A. D. Becke, *J. Chem. Phys.* **1993**, *98*, 5648.
[10] R. J. Bartlett, *Annu. Rev. Phys. Chem.* **1981**, *32*, 359.
[11] K. Raghavachari, G. W. Trucks, J. A. Pople, M. Head-Gordon, *Chem. Phys. Lett.* **1989**, *157*, 479.
[12] a) C. Peng, H. B. Schlegel, *Isr. J. Chem.* **1993**, *33*, 449; b) C. Peng, P. Y. Ayala, H. B. Schlegel, M. J. Frisch, *J. Comput. Chem.* **1996**, *17*, 49.
[13] M. J. Frisch, J. A. Pople, J. S. Binkley, *J. Chem. Phys.* **1984**, *80*, 3265.
[14] Gaussian 94, Revision C.3, M. J. Frisch, G. W. Trucks, H. B. Schlegel, P. M. W. Gill, B. G. Johnson, M. A. Robb, J. R. Cheeseman, T. Keith, G. A. Petersson, J. A. Montgomery, K. Raghavachari, M. A. Al-Laham, V. G. Zakrzewski, J. V. Ortiz, J. B. Foresman, J. Cioslowski, B. B. Stefanov, A. Nanayakkara, M. Challacombe, C. Y. Peng, P. Y. Ayala, W. Chen, M. W. Wong, J. L. Andrés, E. S. Replogle, R. Gomperts, R. L. Martin, D. J. Fox, J. S. Binkley, Defrees, D. J. J. Baker, J. P. Stewart, M. Head-Gordon, C. Gonzales, J. A. Pople, Gaussian94-Revision D.3, Gaussian, Inc., Pittsburgh PA, **1995**.
[15] a) S. G. Lias, J. E. Bartmess, J. F. Liebman, J. L. Holmes, R. D. Levin, W. G. Mallard, *J. Phys. Chem. Ref. Data* **1988**, 17, Suppl. 1; b) NIST Chemistry Webbook.nist (http://webbook.nist.gov/chemistry) NIST Standard reference Database n. 69, March **1998** release.
[16] F. Cacace, G. de Petris, F. Pepi, M. Rosi, A. Sgamellotti, *Angew. Chem.* **1999**, *111*, 2555; *Angew. Chem. Int. Ed.* **1999**, *38*, 2408.
[17] a) L. T. Molina, M. J. Molina, *J. Phys. Chem.* **1987**, *91*, 433; b) L. M. Arin, P. Warneck, *J. Phys. Chem.* **1972**, *76*, 1514.
[18] a) F. Cacace, R. Cipollini, G. de Petris, F. Pepi, M. Rosi, A. Sgamellotti, *Inorg. Chem.* **1998**, *37*, 1398; b) F. Cacace, G. de Petris unpublished results.

Received: November 9, 1999 [F2127]

  0947-6539/00/0614-2581 $ 17.50+.50/0